

Surprises in the Structural Chemistry of Zeolites*

J. M. THOMAS

AND (IN PART) S. RAMDAS, G. R. MILLWARD, J. KLINOWSKI,
M. AUDIER, J. GONZALEZ-CALBET, AND C. A. FYFE†

*Department of Physical Chemistry, University of Cambridge, Cambridge
CB2 1EP, United Kingdom*

Received December 4, 1981

High-resolution electron microscopy, apart from strikingly confirming the correctness of the X-ray-based models for the skeletal structure of the aluminosilicate frameworks of zeolites, points to the existence of new families of ordered, crystalline microporous solids (e.g., with composition $A_x B_x C_{m-x} O_{2m} \cdot nH_2O$, where A is an exchangeable monovalent cation, B is Al or Ga, C is Si or Ge, and x, m, n are integers.) It also reveals crystalline imperfections and unexpected superlattice structures in A -type and faujasitic zeolites, and the nature of the intergrowths in, for example, ZSM-5/ZSM-11 materials. The short-range order of Si and Al within the aluminosilicate framework may be directly explored by magic-angle-spinning NMR (MASNMR) employing ^{29}Si and ^{27}Al nuclei. This technique probes the site symmetry and environment of these atoms. Al in tetrahedral as well as in octahedral sites may be readily identified and so may the populations of groups such as $\text{Si}(\text{OAl})_4$, $\text{Si}(\text{OAl})_3$, (OSi) , etc., so that new information is obtained pertaining to Si,Al ordering in a variety of zeolitic solids.

1. Introduction

In 1942 a paper by Wells and co-workers (1) showed that, in the solid state, phosphorus pentachloride is an ionic not a molecular crystal, as one might have expected on the basis of its formula PCl_5 . It is composed not of trigonal bipyramidal entities as in the gas phase but of PCl_4^+ and PCl_6^- ions and possesses essentially the cesium chloride structure. This somewhat surprising result serves as an elegant pedagogic illustration of how a change of state is sometimes accompanied by a significant change

in structure. It also forewarns us of later surprises such as the occurrence of the "compound" PBr_7 (i.e., $\text{PBr}_4^+ \cdot \text{Br}_3^-$) which, superficially at least using the rudiments of valence theory, would have appeared puzzling.

All this was accomplished through the agency of X-ray crystallography, one of the most useful structural tools then, as now, at the chemist's disposal.¹ At that time NMR

¹ Consultation of the original paper by Clark, Powell, and (independently) A. F. Wells (1) is an unusually evocative and instructive experience. It highlights the changes and advances that have taken place in the 40 years that have elapsed since its submission. Crystals were prepared (in this University) by distilling the substance in a vacuum into a Lindemann glass tube, and Weissenberg photographs of these provided sufficient data for a preliminary determination of the structure. At Oxford, better quality single crystals were obtained from nitrobenzene solution. They were

* Dedicated to Professor A. F. Wells on his 70th birthday.

† Present address: Guelph-Waterloo Centre for Graduate Work in Chemistry, University of Guelph, Ontario N1G 2W1, Canada.

had not been discovered; but for a long time after its discovery NMR was applied chiefly, and extraordinarily successfully, by organic chemists to the elucidation of structures in the fluid state. Indeed not until very recently (4–8) has NMR been used in such a way as to extract direct structural information from solids which, for one reason or another, prove intractable to study by X-ray diffraction and allied techniques. This is accomplished by rapid specimen rotation about an axis inclined at the “magic angle” of $54^{\circ}44'$ (half the tetrahedral angle) to the direction of the applied magnetic field. Since there is a term $(3 \cos^2\theta - 1)$ in the expression for the broadening of the resonance in the signal from the solid, and since this term is zero at $\cos \theta = (1/3)^{1/2}$, it can be seen how a spectral line in a solid may be drastically reduced by rapidly spinning the specimen at the “magic angle” to the external magnetic field. By recording solid-state NMR spectra in this way, rather revealing chemical-shift information comes to light, comparable to that obtained, and already extensively exploited, in the liquid state. Fuller details of the technique are given in a recent review by Andrew (5), one of the founders of MASNMR (magic-angle-spinning NMR).

The ^{31}P MASNMR spectrum of rapidly rotated crystalline phosphorus pentachloride is shown in Fig. 1. For the stationary solid, the spectral line width is in the kilohertz range: the MASNMR spectrum, however, consists of two well-resolved lines re-

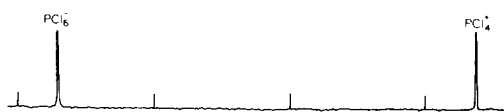


FIG. 1. The solid-state ^{31}P spectrum (MASNMR) of polycrystalline phosphorus pentachloride. The two lines arise from the PCl_4^+ and PCl_6^- ions of which the solid (see Ref. (1)) is composed. Reproduced, with permission, from Ref. (5).

duced to 10-Hz breadth. By contrast, the same material, when dissolved in CS_2 , yields a single sharp line attributable to the molecular entity PCl_5 .

The above spectrum underlines the potential importance of MASNMR as a new structural tool, applicable especially to finely crystalline solids (for which X rays are not, in general, well suited) and applicable also to single-crystal materials composed of atoms of roughly comparable X-ray scattering power. In succeeding sections we show how ^{29}Si and, more recently, ^{27}Al MASNMR have uncovered several new features pertaining to the structural chemistry of the zeolitic aluminosilicates. It will emerge that this is a new method (7–17) for ascertaining Si,Al ordering in anionic, zeolitic frameworks; and it is this ordering that crucially governs the adsorptive capacity, catalytic activity, and acidity of any particular zeolite. We shall focus principally, but not exclusively, upon faujasite-based zeolites.

Another potentially important new structural tool for the study of zeolites (and indeed silicates generally) is that of high-resolution electron microscopy (HREM) (18–23). This, in essence, entails recording the projected structure, or a faithful picture of the projected structure, at near-atomic resolution in real space. Comprehensive, recent reviews, which deal with the reliability, scope, and limitations of the technique are given elsewhere (18–20, 23). It will be shown below that many unexpected aspects of the structure of faujasite-based zeolites (X and Y) as well as of the so-called

coated with “a warm mixture of medicinal paraffin and vaseline which on cooling formed a thin, more or less solid coating capable in favourable cases, of preserving the crystal for a few days.” Overlapping 15° oscillation photographs were taken about the [001] and [100] axes. Intensities were estimated visually. The absence of vertical planes of symmetry was proven by the appearance of pyramidal etch pits on (001)—a technique now known occasionally to yield not altogether unambiguous conclusions in view of the dependence (2, 3) of etch pit shape and orientation on the etchant and the etching conditions.

porotectosilicates, including the renowned catalysts for the conversion of methanol to gasoline, ZSM-5 and ZSM-11, have been brought to light by HREM.

2. A Cherished Guideline: Loewenstein's Rule

In discussions of zeolite structure the veracity of Loewenstein's rule, which forbids sharing of an oxygen atom by two tetrahedrally coordinated Al atoms, has for so long been taken for granted that there is now a tendency to regard as inviolable what was initially intended as no more than a working hypothesis. In essence this rule stipulates that two aluminate tetrahedra (AlO_4^{5-}) cannot share a corner in the way that two silicate tetrahedra (SiO_4^{4-}) can. Yet, both outside and close to the realm of zeolitic solids, there are well-documented examples in which tetrahedral frameworks are made up entirely of (AlO_4^{5-}) units: such is the case in KAlO_2 and in the all-aluminum analogs (24, 25) of sodalite, e.g., $\text{Ca}_8(\text{Al}_{12}\text{O}_{24})(\text{SO}_4)_2$. Furthermore, in bicchulite (26), $\text{Ca}_2\text{Al}_2\text{SiO}_6(\text{OH})_2$, which is another sodalite analog, there have to be some Al–O–Al linkages since $\text{Si}/\text{Al} = 0.5$. In all these examples Loewenstein's rule is broken, yet in many discussions of zeolitic structures the rule often tends to be regarded as axiomatic.

If the rule were strictly obeyed it would follow that in zeolites possessing a Si/Al ratio of unity each central Si would be surrounded, via oxygen, by four Al atoms; i.e., $\text{Si}(4\text{Al})$ units² (so-called 4:0 ordering) would repeat themselves three dimensionally. If it is broken, however, some Al–O–Al links as well as Si–O–Al links must occur, and this would indeed be the case if the repeat units were $\text{Si}(\text{OAl})_3(\text{OSi})$ (i.e., 3:1 ordering). It has been shown elsewhere (7–11) that 4:0, 3:1, 2:2, 1:3, and 0:4

² By $\text{Si}(\text{Al})$ we mean $\text{Si}(\text{OAl})_4$; likewise $\text{Si}(3\text{Al})$ means $\text{Si}(\text{OAl})_3(\text{OSi})$ and so on.

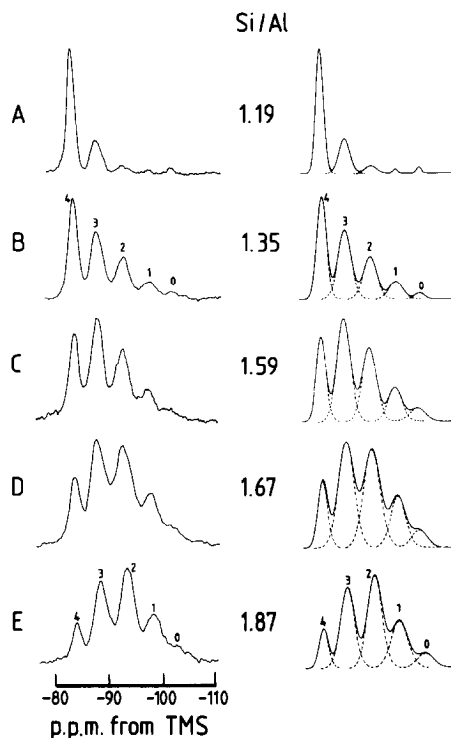


FIG. 2. Typical high-resolution ^{29}Si MASNMR spectra (left) for a range of synthetic faujasitic (Si/Al ratios from 1.19 to 1.87). On the right are given the computer-simulated spectra, based on Gaussian peaks; the dotted lines delineate the deconvolution. The five distinct kinds of primary environment surrounding a central Si atom (i.e., $\text{Si}(4\text{Al})$, $\text{Si}(3\text{Al})$, etc.) are clearly seen and are labeled in spectra B and E. Reproduced, with permission, from Ref. (14).

ordering schemes, corresponding respectively to $\text{Si}(4\text{Al})$, $\text{Si}(3\text{Al})$, $\text{Si}(2\text{Al})$, $\text{Si}(1\text{Al})$, and $\text{Si}(4\text{Si})$ linkages, may be identified by MASNMR; and Fig. 2 shows a series of typical MASNMR spectra reported by Klinowski *et al.* (14) for a range of faujasite-based zeolites (Fig. 3) where the Si/Al ratios cover a range embracing the so-called X-type $\text{Si}/\text{Al} = 1$ to 1.5) and Y-type zeolites ($\text{Si}/\text{Al} > 1.5$). We shall return later (Section 5) to the precise significance of the intensity variations of these peaks as a function of Si/Al ratio, and the information they convey regarding extended ordering of Si and Al. At present we concentrate on whether

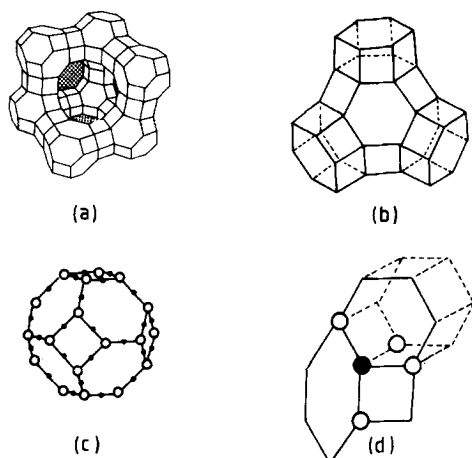


FIG. 3. Framework features of the faujasite structure. The individual cuboctahedra (c), composed of either SiO_4^{4-} or AlO_4^{5-} tetrahedra at each vertex, are linked by hexagonal prisms. Each cuboctahedron is joined to four others: for clarity only three of the four are shown in (b). A schematic representation of the immediate environment of a tetrahedral atom (Si or Al) is shown in (d), where, for heuristic purposes a central aluminum (\bullet) is shown tetrahedrally coordinated (via oxygens) to four silicon atoms (\circ).

Loewenstein's rule is obeyed for the zeolites that we have so far studied.

Figure 2 clearly shows that, for the faujasite structure, as the Si/Al ratio approaches unity the ordering converges toward Si(4Al), i.e., toward strict alternation of Si and Al in the lattice, thus demonstrating that Loewenstein's rule is obeyed. There is another, quite independent (13, 14) proof that Loewenstein's rule is obeyed in faujasite-based zeolites (X and Y). It, too, comes from MASNMR studies. If this rule holds, it follows that the first-order neighborhood of every Al atom is Al(4Si) so that each Si-O-Al linkage in a Si(n Al) structural unit is equivalent to $\frac{1}{4}$ Al atoms. If $I_{\text{Si}(n\text{Al})}$ denotes the MASNMR intensity of a resolvable³ Si(n Al) peak, it follows that the Si/Al ratio is given by

$$(\text{Si}/\text{Al})_{\text{MASNMR}} = \frac{\sum_{n=0}^4 I_{\text{Si}(n\text{Al})}}{\sum_{n=0}^4 0.25nI_{\text{Si}(n\text{Al})}}$$

Table I shows that the agreement between ratios determined this way and by other analytical techniques (X-ray fluorescence, or electron beam-induced X-ray emission) is good.

3. Do Any Zeolites Violate Loewenstein's Rule?

On the basis of MASNMR spectra recorded for a series of zeolites that possess a Si/Al ratio close to unity it has been concluded that, because the primary Si spectral feature was an intense peak, attributed to Si(3Al), Loewenstein's rule is broken and Al-O-Al linkages are, therefore, thought to occur in such solids (Table II). The zeolites believed to fall into this category are Losod, Linde A, sodalite, and cancrinite. Lippmaa *et al.* (8) offer evidence to indicate

TABLE I
COMPARISON OF Si/Al RATIOS
IN ZEOLITES X AND Y
MEASURED USING X-RAY
FLUORESCENCE (XRF) AND
CALCULATED FROM SOLID
STATE ^{29}Si MASNMR
SPECTRA

$(\text{Si}/\text{Al})_{\text{XRF}}$	$(\text{Si}/\text{Al})_{\text{NMR}}$
1.19	1.14
1.35	1.39
1.59	1.57
1.67	1.71
1.87	1.85
2.00	1.98
2.35	2.46
2.56	2.69
2.61 ^a	2.56
2.75	2.69

³ Intensities may be quantitatively determined by accurate deconvolution of spectrally well-resolved Gaussian peaks.

^a By energy-dispersive X-ray analysis (EDA) using electron microscopy.

TABLE II
ZEOLITIC SOLIDS IN WHICH, ON THE BASIS OF
MASNMR STUDIES, LOEWENSTEIN'S RULE IS
THOUGHT TO BE VIOLATED^a

Zeolite	Idealized formula	Si,Al ordering scheme ^b
Sodalite	Na ₆ Al ₆ Si ₆ O ₂₄ · 8H ₂ O	3:1 ^c
Losod	Na _{11.5} Al ₁₂ Si ₁₂ O ₄₈ · 17.8H ₂ O	3:1
Linde A ^d	Na ₁₂ Al ₁₂ Si ₁₂ O ₄₈ · 27H ₂ O	3:1
Cancrinite hydrate ^e	Na ₆ Al ₆ Si ₆ O ₂₄ · 6H ₂ O	3:1 ^f

^a After Ref. (9).

^b The basis of the decision concerning Si:Al ordering rests on the currently accepted ²⁹Si₉ chemical shift ranges. For 4:0 it is believed to extend from -88 to -87 ppm (from Me₄Si); for 3:1 from -88 to -95. More "known" aluminosilicate structures need to be studied to determine the reliability of these limits.

^c Other samples of sodalite are thought to exhibit 4:0 ordering, and in these, unlike those that have 3:1 ordering, Al-O-Al links are not unavoidable.

^d To date, a wide range of cation-exchanged forms of zeolite A (Na⁺, K⁺, Ag⁺, Tl⁺, Ca²⁺, Mg²⁺, and La³⁺) have all been shown to yield a single ²⁹Si resonance at -88.5 ± 0.5.

^e Synthesized according to J. WYART, *Discuss. Faraday Soc.* 5, 323 (1949).

^f As with sodalite, some samples of cancrinite seem to exhibit 4:0 ordering.

(See note Added in Proof at end of article.)

that in gmelinite (Si/Al = 2) Loewenstein's rule is also violated. There has been some evidence to suggest that, depending on the provenance of a particular specimen, the ordering scheme in the aluminosilicate framework in question may be either 4:0 or 3:1. Very recently, there have been some indications that it may be possible for other zeolites (27), including Linde A perhaps (contrary to what was originally thought), to adopt two or more distinct ordering schemes within a given preparation. MASNMR evidence points to this, in that distinct Si(4Al) and Si(2Al) peaks may be discerned on either side of the dominant Si(3Al) peak, although these features have to be interpreted with care as they may

arise from traces of other zeolitic impurities. Moreover, electron diffraction patterns (such as that shown in Fig. 8 of Ref. (28)) clearly indicate that local Si,Al order may be very different from that which predominates in the remainder of the sample.

At first sight it seems implausible that a 3:1 rather than a 4:0 ordering scheme should be adopted by any zeolite with Si/Al of unity. The 4:0, strictly alternating SiO₄⁴⁻/AlO₄⁵⁻ structure for Linde A, has an intrinsic simplicity that rings true (28). But deeper analysis shows that this may be energetically less favored in Linde A than the superficially less plausible 3:1 ordering scheme involving Si(O-Al)₃(O-Si) repeat units. It can be shown, on the basis of a simple approximation which focuses entirely on the repulsions between intraframework Al³⁺ ions, that the 3:1 model rivals the 4:0 model so far as the energetics of the Linde A structure are concerned. More rigorous calculations (29) carried out both by Catlow and by Engelhardt and their colleagues on dehydrated A zeolite structures with known competing models (3:1 versus 4:0), come out distinctly in favor of the 3:1 scheme (see Table III).

Our approximate method also shows that for faujasite a 4:0 ordering scheme rather than a 3:1 scheme is energetically preferred, and that, for sodalite (see below) as with zeolite A, there is only a small difference in intraframework repulsion energy

TABLE III
CALCULATED ENERGIES OF THE *R* $\bar{3}$ AND *Fm*3*c*
MODELS OF THE STRUCTURE OF DEHYDRATED
Na-A ZEOLITE^a

	Energy (eV)	
	<i>R</i> $\bar{3}$	<i>Fm</i> 3 <i>c</i>
Reported structural coordinates	-107.682	-106.942
Minimized structure	-109.363	-107.603

^a After Ref. (29).

for the 4:0 and 3:1 schemes. Furthermore, the rigorous approach of Catlow *et al.* (29) shows how sensitively the location of the exchangeable cation affects the overall energy. It seems that a given ordering scheme, and, in particular, one which entails Al–O–Al– linkages, may be greatly stabilized if the cations are brought close to these linkages: this is the conclusion drawn by Catlow *et al.* and by Engelhardt (29).

4. The Enigma of Zeolite A

Up until work began a few years ago using MASNMR, HREM electron diffraction, and neutron (powder) diffraction, the strictly alternating (4:0) structure (space group $Fm\bar{3}c$) for zeolite A (30, 31) was widely accepted. There are, however, various reasons (summarized elsewhere) (28, 32, 33) based on combined electron diffraction, MASNMR, and neutron diffraction (34) studies for reexamining the correctness of this structure. An alternative model (28) involving repeat unit (a) rather than repeat unit (b) (Fig. 4) satisfies all the known recorded experimental information for Na–A zeolite specimens (of Si/Al = 1.00 ± 0.02) prepared by us. Note that a rhombohedral distortion (that had escaped detection in previous X-ray crystallographic studies leading to an assignment of a rhombohedral space group $R\bar{3}$) is associated with the repeat unit depicted in Fig. 4b. Very recently, however, neutron diffraction powder data (27) have been collected by us from Tl–A and Ag–A zeolites, and it is clear that the rhombohedral distortion, if present at all (for specimens possessing Si/Al ratio greater than unity), is vanishingly small and not detectable with neutron wavelengths of 2.96 Å. The MASNMR spectra, however, still yield a single resonance interpreted as due to 3:1 rather than 4:0 ordering, yet refinement of the neutron data is proceeding smoothly in space group $Fm\bar{3}c$ and sensible Si–O and

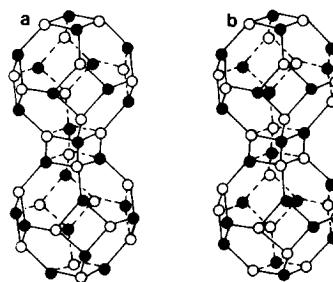


FIG. 4. Representation of the asymmetric units (of Na–A zeolite) for the space groups $Fm\bar{3}c$ and $R\bar{3}$. Filled and open circles represent Al and Si atoms, respectively. In (a) there is 4:0 ordering, and in (b), 3:1 ordering of the Si, Al atoms. (After Ref. (28).)

Al–O bond distances are derived in this way. The enigma, therefore, amounts to this: the Si,Al ordering, as gauged by MASNMR is 3:1 yet the $Fm\bar{3}c$ space group, which implies a 4:0 scheme, yields satisfactory bond lengths in the two distinct tetrahedra. Furthermore, it is now clear that significant rhombohedral distortion is not an inevitable consequence of a 3:1 ordering scheme. More work, currently in progress, on the MASNMR of “high-silica” analogs of zeolite A and on neutron scattering of other cation-exchanged A samples, is required to eliminate this enigma. It is clear that the specific remarks of Bursill *et al.* (28) in their discussion of zeolite A need now to be actively pursued: “It is therefore felt that further analysis of possible cubic structures, or a statistical mixture of cubic and rhombohedral structures, is not warranted at present. If the refinement of the $R\bar{3}$ structure, with varying Si/Al ratio, is not entirely successful for all samples (of zeolite A) then it may be necessary to reconsider the situation.” (See Note Added in Proof.)

5. Si,Al Ordering in Zeolites X and Y

With the aid of spectra of the kind shown in Fig. 2, from which accurate intensities of specific groupings (Si(4Al), Si(3Al), etc.) may be read off, and with additional argu-

ments based on crystal symmetry and electrostatic energy (see Refs. (10) and (14)), it is possible to arrive at specific models for the ordering of Si and Al within the aluminosilicate framework. Typical examples of our derived models for faujasite-based zeolites with Si/Al ratios of 1.00 and 3.00 are shown, respectively, in Figs. 5 and 6. These conclusions are broadly in agreement with those of other workers (13, 35) who have employed MASNMR.

In ZSM-5 and silicalite the Si/Al ratio is very large, and it becomes difficult to evaluate the ordering schemes unambiguously. We have recently shown however that, in silicalite, the aluminum is tetrahedrally bound (quite a surprise!). We can also resolve very many crystallographically distinct Si(OSi)₄ sites in silicalite.

6. Si,Al Ordering in Sodalite

One of the surprises to emerge from studies (by MASNMR) of various types of synthetic and natural sodalites (8, 9, 12, 35) is the suggestion that sometimes 4:0 and sometimes 3:1 ordering occurs. (The same appears to be true of cancrinite (9).) Though much confirmatory work, using electron, X-ray, and neutron diffraction needs to be carried out, one may readily imagine how the well-known sodalite

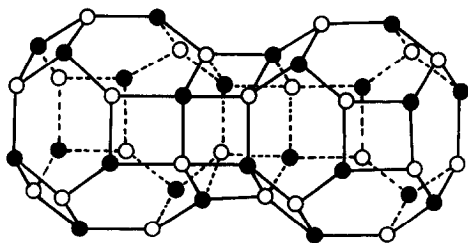


FIG. 5. The most likely Si, Al ordering scheme in zeolite X (i.e., faujasite with Si/Al = 1.0) based on the predicted ²⁹Si MASNMR intensity ratio for the five peaks and the observed trend in the intensity ratios as Si/Al decreases (see Fig. 2) (see Ref. (14) for further details).

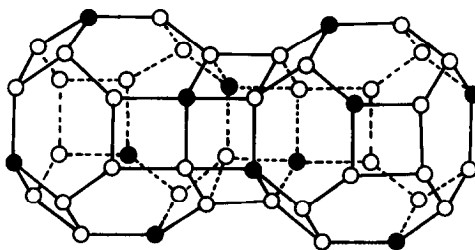
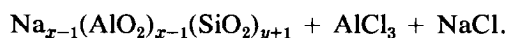


FIG. 6. The most likely (14) Si,Al ordering scheme in zeolite Y with Si/Al = 3.0.

framework can accommodate long-range order on the 3:1 local ordering principle. It transpires that there are two distinct ways in which this kind of Si(3Al) grouping may be translationally repeated in three dimensions (Fig. 7).

7. Manipulating the Faujasite Structure

It has been discovered (11, 36) that dealumination of faujasite may be smoothly effected by exposing the dry Na-exchanged solid at elevated temperatures (150 to 450°C), in either a fixed or a fluidized bed, to SiCl₄ vapor for a few hours. Aluminum is successively substituted in the zeolitic framework by silicon, and removed from the crystals in the form of volatile AlCl₃:



After the dealuminated faujasite is flushed with either dry nitrogen or dry argon and the temperature is gradually reduced, the

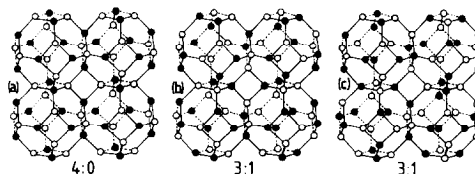


FIG. 7. Schematic illustration showing how the sodalite framework may in principle, accommodate both 4:0 and 3:1 ordering of two distinct kinds b and c. Diffraction studies should be able to distinguish (b) and (c) if, indeed, these variants do exist.

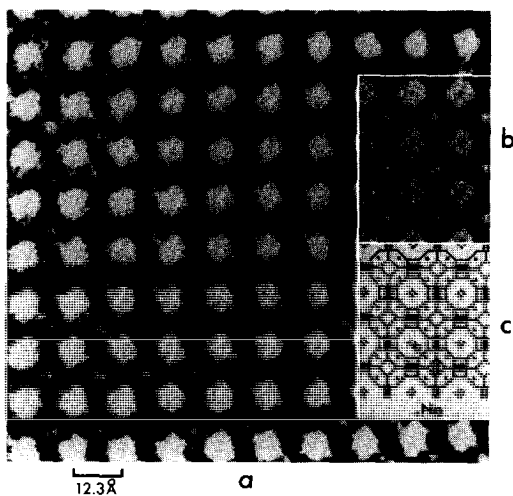


FIG. 8. High-resolution electron microscopic image (a) of a dehydrated crystal (ca. 50 Å thick) of Na-A zeolite viewed along [100]. The insets show the computer-simulated image (b) and a simplified scalar drawing (c) of the structure in which the Na ions are denoted by small circles. Both the large (so-called α cages) as well as the small β cages (i.e., those at the centers of cuboctahedra) are visible. The centers of adjacent cages are 12.3 Å apart.

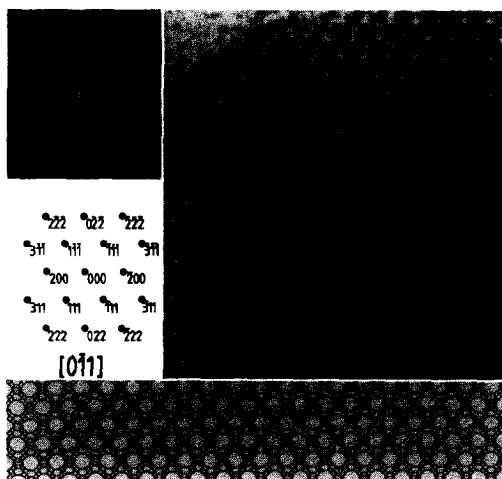


FIG. 9. A typical high-resolution image and corresponding diffraction pattern, with scalar drawing of the faujasitic zeolites (Na-Y or La-Y) viewed along $\langle 110 \rangle$. Exchangeable cations not shown. Large white spots in micrograph correspond to supercages.

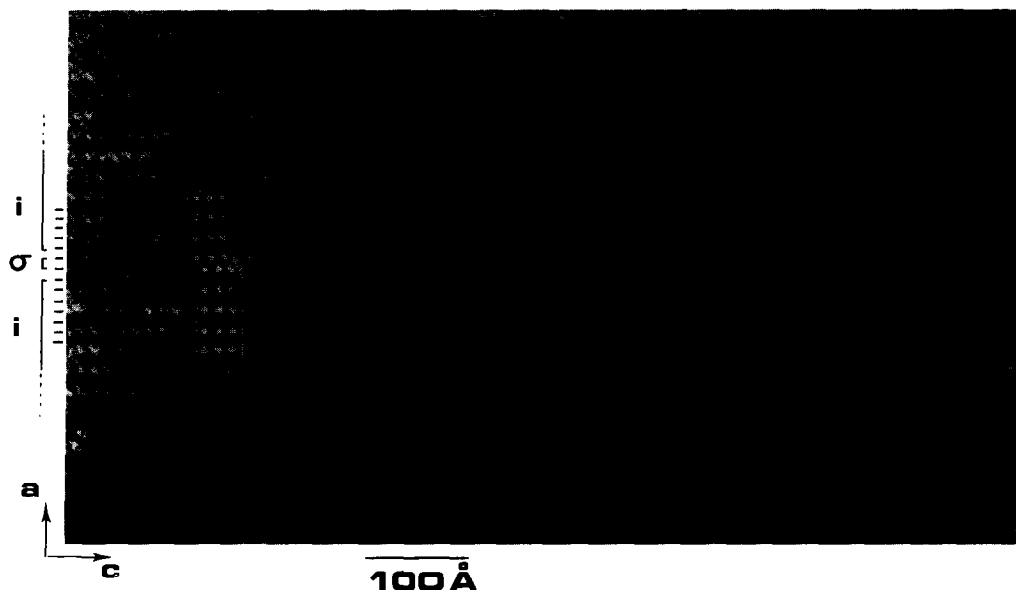


FIG. 10. High-resolution image showing an intergrowth of ZSM-5 and ZSM-11. The interpretation is based on the occurrence of an image defect caused by multiple scattering of electrons within the specimen. For the 010 projection of ZSM-5, this scattering results in the usual triangular lattice of white spots (representing channels) being replaced by a rectangular lattice where intervening spots have lost intensity. This effect does not occur for ZSM-11. The change in phase of the rectangular lattice (on proceeding from top to bottom of ZSM-5) is consistent with a change of symmetry along [100] planes arising from inversion (i) to mirror, (σ) at one (but no more) of the planes marked σ , thus yielding a small strip of ZSM-11.

resulting "silica"-rich (Si/Al ratio >50) product is washed to remove any residual material. Surprisingly, and very conveniently as the resulting silica-rich analog of faujasite is a good, novel catalyst (11), there is almost complete retention of the structural integrity, as revealed by HREM and X-ray diffraction. Significantly, the ^{27}Al MASNMR spectrum of dealuminated zeolite Y contains two peaks: one due to residual aluminium still on tetrahedral sites and an additional peak arising from octahedrally coordinated aluminum on cationic positions in the zeolitic channels. The latter can be removed by thorough washing, whereupon the intensity of the octahedral peak is diminished.

8. Views of Zeolite Structures at Near-Atomic Resolution (by HREM)

Thanks largely to the efforts of Audier, Bursill, Gonzalez-Calbet, and Millward (21, 22, 37-42) in these Laboratories, it is now possible to record projected images at near-atomic resolution of most zeolitic solids. A few, such as natrolite, scolecite, and mordenite, remain intractable; but the majority selected for study so far can be imaged albeit under conditions which, by the normal standards (20) of high-resolution electron microscopy, are adverse. Figures 8 and 9 show typical high-resolution images of zeolite A and zeolite Y along high-symmetry directions. These are unsurprising, except inasmuch as they offer striking proof for the correctness of X-ray-derived skeletal structure: the gaps (α -, β -, and super-cages) are clearly visible. Structural imperfections (see Figs. 2 and 3 of Ref. (37)), coherent intergrowths (see Fig. 7 of (21) and Fig. 10), multiple twinning (Fig. 11), and unexpected superlattices (Fig. 12) have been directly "seen" using HREM, and the information has added new dimensions to our knowledge of the ultrastructure of zeo-

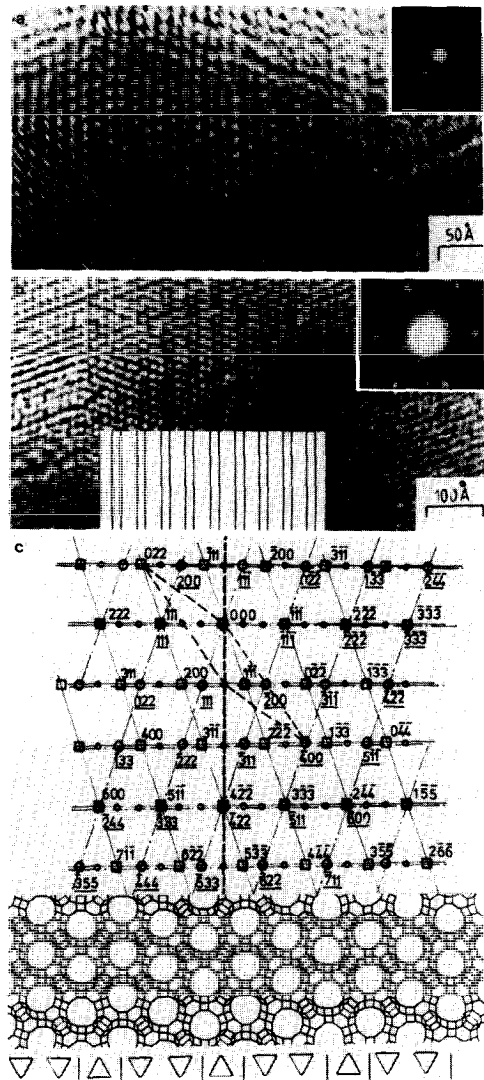


FIG. 11. High-resolution images (a) and (b) of multiply twinned zeolite Y. In (a) inset shows the corresponding electron diffraction pattern; in (b) inset shows the corresponding optical diffraction pattern of the image (additional inset identifies twin planes). (c) Interpretation of the electron diffraction pattern: extra spots, shown as unindexed small circles, arise from double diffraction. Thick vertical broken line demarcates twin plane. The framework drawing shows twinned zeolite along $\langle 110 \rangle$. Matrix and twin are symbolized by \triangle and ∇ , respectively, and small slashes represent twin planes.

lites. We shall trace the significance of but one of these features here, that of recurrent

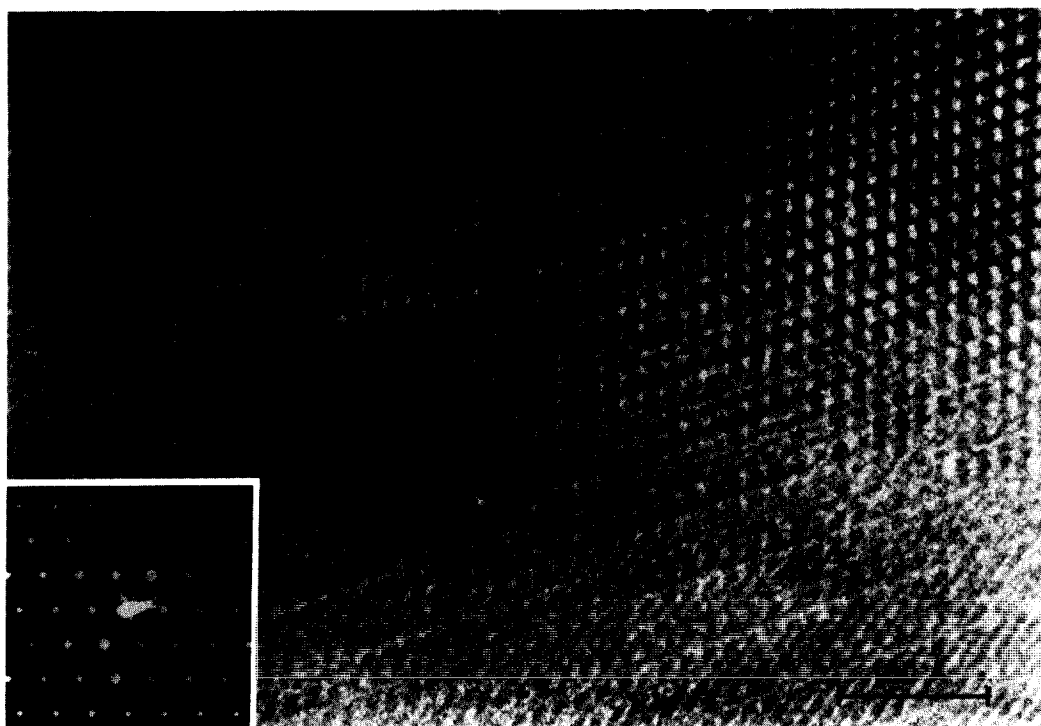


FIG. 12. High-resolution image and corresponding diffraction pattern (inset) showing threefold superlattices along $\langle 111 \rangle$. Both Na^+ -exchanged and K^+ -exchanged zeolite Y specimens display these tendencies (which also appear to be dependent upon the Si/Al ratio).

twinning on $[111]$ planes in the faujasite-based zeolites X and Y.

9. Discovery of a New Family of Crystalline Microporous Structures

Figure 13 demonstrates the reality of recurrent twinning on $\{111\}$, even though the extent of the twinning is not pronounced. The effect of inserting two consecutive twin planes into the faujasite structure is illustrated in Fig. 13. The parent structure (see Fig. 3), which consists of an array of "supercages," each with a free diameter of ca. 13 \AA , separated by apertures with a diameter of 7.4 \AA , is converted by recurrent twinning into a tunnel structure. The diameter of the tunnel varies between 7.4 and 13 \AA . Intersecting these tunnels which run along $\langle 111 \rangle$ are apertures which are elliptical with

dimensions 6.9 and 7.4 \AA . The new structure is hexagonal. Figure 14 emphasizes the essential changes in connectivity of the cub-octahedra at the twin plane. The regular, untwinned faujasite structure may be represented by $\dots \Delta\Delta\Delta\Delta \dots$, where each Δ denotes a building unit repeat along $\langle 111 \rangle$ (i.e., 14.2 \AA). The sequence $\dots \Delta/\nabla/\Delta/\nabla/\Delta \dots$ signifies that a twin lamella, ∇ , bounded by a pair of $\{111\}$ twin planes, denoted by slashes, is inserted along every alternate unit cell repeat along $\langle 111 \rangle$. If the number of twin planes introduced in this way is n , the length of the tunnel in the new structure is $14.2 \times (n + 1) \text{ \AA} + 6.95 \text{ \AA}$. The second term in the sum accounts for twice the distance between the extreme (111) plane and the wall of the supercage, with which the tunnel terminates at each end. (The new structure described here has a

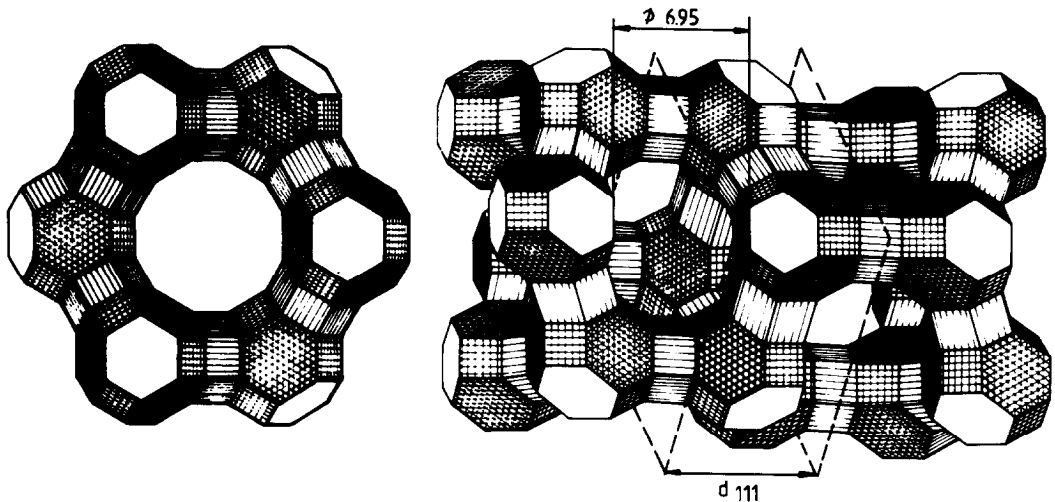


FIG. 13. The faujasite structure (right) with two consecutive $[111]$ twin planes, denoted by dashed lines. The view along $[111]$ of the twinned structure is shown on the left.

certain kinship with, but is distinct from, the so-called structure 6 discussed as a theoretical possibility by Breck (43). It is the same as the structure proposed by A. F. Wells, as a theoretical possibility, in his text on structural inorganic chemistry.) A sequence such as . . . $\Delta\Delta/\nabla/\Delta\Delta/\nabla$. . . signifies that a twin lamella is introduced between flanking pairs of regular repeat units along $\langle 111 \rangle$. This gives rise to a new structure composed of interconnected "hypercages" which are 49.6 Å in length and a diameter which again varies between 13 and 7.4 Å.

Recognizing that, as discussed above, the Si/Al ratio in a faujasitic zeolite may range from 1.0 to beyond 100; that Ga and In may enter the tetrahedral sites occupied by Al and Ge, and Sn may enter the tetrahedral sites occupied by Si; and that there are ways of boosting the degree of recurrent twinning in synthetic faujasites (42, 44), it can be seen that new families of crystalline, three-dimensionally ordered microporous structures may be engineered (44) from zeolitic precursors. With the faujasite precursor such solids would have a composition $A_x B_x C_{m-x} O_{2m} \cdot nH_2O$, where A is an

exchangeable monovalent cation, B is typically Al or Ga, C is typically Si or Ge, and x , m , and n are integers the magnitudes of which are governed by the size of the unit cell. These solids possess unusual but desirable structures in that they have tunnel diameters of molecular dimension. It re-

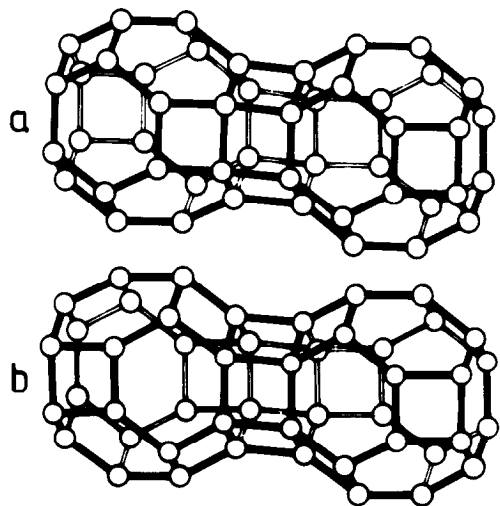


FIG. 14. The essential difference between the un-twinned (a) and twinned (b) faujasite structures of the aluminosilicate framework. In (b) the twin plane is perpendicular to the paper and intersects the hexagonal prism.

mains to be seen whether convenient methods exist for scaling up the production of such intriguing new materials.

Acknowledgments

We acknowledge stimulating discussions with Drs. M. Barlow, L. A. Bursill, D. A. Jefferson, D. Stewart, and D. Young.

Note added in proof (July 1982). As a result of discoveries made (45–50) since this work was submitted it is now clear that zeolite-A has 4:0 not 3:1 ordering (i.e., the Si, Al distribution is as shown in Fig. 4a not as in Fig. 4b). ^{29}Si MASNMR, the technique that first called into question the ordering scheme deduced by X-ray methods (31), is also responsible for the reaffirmation of the original, 4:0 scheme. We have described in detail elsewhere (45) how the ^{29}Si MASNMR spectra of ZK-4 zeolites (Si/Al ratios 1.6 to 1.8) confirm the 4:0 ordering scheme. Briefly, the argument is based on the fact that all five distinct $\text{Si}(\text{OAl})_4-n(\text{OSi})_n$ peaks exhibited by ZK-4 (which has the same framework structure as Linde-A) can be assigned unambiguously, and, in particular, the peak at -88.6 p.p.m. is shown to correspond to $\text{Si}(\text{OAl})_4$. This means that the range of shifts for the $\text{Si}(\text{OAl})_4$ grouping is broader than what was originally believed (7, 9). We have shown (45) that, as the T–O–T angle in a zeolite increases, the ^{29}Si resonance for a given functional grouping is shifted to more negative values.

Rietveld profile analysis of neutron powder diffraction data of TI-A enable the Si, Al ordering to be determined directly in that structure (49); the Si, Al ordering and cation positions have also been determined in ZK-4 (50).

References

1. D. CLARK, H. M. POWELL, AND A. F. WELLS, *J. Chem. Soc.* 643 (1942).
2. J. J. GILMAN AND W. G. JOHNSTON, *Solid State Physics* 13, 148 (1962).
3. J. M. THOMAS AND G. D. RENSHAW, *Trans. Faraday Soc.* 61, 791 (1965).
4. *Phil. Trans. R. Soc. London Ser. A* 299, 475–689 (1981) Special issue (R. Richards and K. J. Packer, Eds.).
5. E. R. ANDREW, *Int. Rev. Phys. Chem.* 1, 195 (1981).
6. C. A. FYFE, W. H. FLEMING, R. D. KENDRICK, J. R. LYERLA, H. VANNI, AND C. S. YANNONI, in "Polymerization Characterization by ESR and NMR" (A. E. Woodward and F. A. Bovey, Eds.), ACS Series, Vol. 142, p. 193, Amer. Chem. Soc., Washington, D. C. (1980).
7. E. LIPPMAA, M. MÄGI, A. SAMOSON, G. ENGELHARDT, AND A-R. GRIMMER, *J. Amer. Chem. Soc.* 102, 4889 (1980).
8. E. LIPPMAA, M. MÄGI, A. SAMOSON, M. TARMAN, AND G. ENGELHARDT, *J. Amer. Chem. Soc.* 103, 4992 (1981).
9. J. KLINOWSKI, J. M. THOMAS, C. A. FYFE, AND J. S. HARTMAN, *J. Phys. Chem.* 85, 2590 (1981).
10. S. RAMDAS, J. M. THOMAS, J. KLINOWSKI, C. A. FYFE, AND J. S. HARTMAN, *Nature (London)* 292, 228 (1981).
11. J. M. THOMAS, G. R. MILLWARD, S. RAMDAS, L. A. BURSILL, AND M. AUDIER, *Faraday Discuss. Chem. Soc.*, No. 72, Paper 20 (Nottingham, Sept. 1981), in press.
12. J. M. THOMAS, J. KLINOWSKI, C. A. FYFE, J. S. HARTMAN, AND L. A. BURSILL, *J. Chem. Soc. Chem. Commun.*, 678 (1981).
13. (a) G. ENGELHARDT, E. LIPPMAA, AND M. MÄGI, *J. Chem. Soc. Chem. Commun.*, 712 (1981); (b) G. ENGELHARDT, U. LOHSE, E. LIPPMAA, M. TARMAN, AND M. MÄGI, *Z. Anorg. Allg. Chem.* 478, 239 (1981); (c) G. ENGELHARDT, U. LOHSE, A. SAMOSON, M. MÄGI, M. TARMAN, AND E. LIPPMAA, *Zeolites*, in press.
14. J. KLINOWSKI, S. RAMDES, J. M. THOMAS, C. A. FYFE AND J. S. HARTMAN, *J. Chem. Soc. Faraday Trans. 2* (1982), in press.
15. C. A. FYFE, G. C. GOBBI, J. S. HARTMAN, J. KLINOWSKI, AND J. M. THOMAS, submitted for publication.
16. D. MÜLLER, W. GESSNER, H-J. BEHRENS, AND G. SCHELER, *Chem. Phys. Lett.* 79, 59 (1981).
17. J. KLINOWSKI, J. M. THOMAS, C. A. FYFE, AND J. S. HARTMAN, *J. Phys. Chem.* 86, 1247 (1982).
18. J. M. THOMAS AND D. A. JEFFERSON, *Endeavour, New Series* 2, 127 (1978).
19. L. EYRING, in "Solid State Chemistry: A Contemporary Overview," ed. (S. L. Holt, J. B. Milstein, and M. Robbins, Eds.), Advances in Chemistry Series 186, p. 27, Amer. Chem. Soc., Washington, D.C. (1980).
20. M. BEER, R. W. CARPENTER, L. EYRING, C. E. LYMAN, AND J. M. THOMAS, *Chem. Eng. News* 59, 40 (1981).
21. J. M. THOMAS, G. R. MILLWARD, AND L. A. BURSILL, *Phil. Trans. R. Soc. London Ser. A* 300, 43 (1981).
22. J. M. THOMAS, *Ultramicroscopy* 8, 13 (1982).
23. J. M. COWLEY, in "Direct Imaging of Atoms in Crystals and Molecules," Proceedings, 47th Nobel Symposium, (L. Khilborg, Ed.), Lidings, Sweden (see also *Phys. Script.* 1978–1979).

24. P. E. HALSTEAD AND A. E. MOORE, *J. Appl. Chem.* **12**, 413 (1962).
25. H. SAALFELD AND N. DEPMEIER, *Krist. Tech.* **7**, 229 (1972).
26. K. SAHL, *Z. Kristallogr.* **152**, 13 (1980).
27. J. M. THOMAS, A. K. CHEETHAM *et al.*, unpublished work.
28. L. A. BURSILL, E. A. LODGE, J. M. THOMAS, AND A. K. CHEETHAM, *J. Phys. Chem.* **85**, 2409, (1981).
29. C. A. A. CATLOW *et al.*, AND G. ENGELHARDT *et al.*, submitted.
30. R. M. BARRER AND W. M. MEIER, *Trans. Faraday Soc.* **54**, 1074 (1958).
31. V. GRAMLICH AND W. M. MEIER, *Z. Kristallogr.* **133**, 134 (1971).
32. J. M. THOMAS, L. A. BURSILL, E. A. LODGE, A. K. CHEETHAM, AND C. A. FYFE, *J. Chem. Soc. Chem. Commun.* **276** (1981).
33. L. A. BURSILL, E. A. LODGE, AND J. M. THOMAS, *Nature (London)* **291**, 265 (1981).
34. E. A. LODGE, Ph.D. Thesis, University of Cambridge (1981).
35. M. MELCHIOR, A. J. JACOBSON, AND D. E. W. VAUGHAN, *J. Amer. Chem. Soc.* **104** (1982), in press.
36. H. K. BEYER AND I. BELENYKAJA, in "Catalysis by Zeolites" (B. Imelik, Ed.), p. 203, Elsevier, Amsterdam (1980).
37. L. A. BURSILL, E. A. LODGE, AND J. M. THOMAS, *Nature (London)* **286**, 111 (1980).
38. L. A. BURSILL, J. M. THOMAS, AND K. J. RAO, *Nature (London)* **289**, 157 (1981).
39. J. M. THOMAS AND L. A. BURSILL, *Angew. Chem. Int. Ed.* **19**, 745 (1980).
40. L. A. BURSILL AND J. M. THOMAS, in "Recent Progress Reports and Discussions: 5th International Conference on Zeolites, Naples, June 1930" (R. Sersale, C. Colella, and R. Aiello, Eds.), p. 25, Giannini, Naples (1981).
41. L. A. BURSILL AND J. M. THOMAS, *J. Phys. Chem.* **85**, 3007 (1981).
42. M. AUDIER, J. M. THOMAS, J. KLINOWSKI, D. A. JEFFERSON, AND L. A. BURSILL, *J. Phys. Chem.*, **86**, 581 (1982).
43. D. W. BRECK, "Zeolite Molecular Series," pp. 56-57, Wiley, New York/London (1974).
44. J. M. THOMAS, M. AUDIER, AND J. KLINOWSKI, *J. Chem. Soc. Chem. Commun.*, 1221 (1981).
45. J. M. THOMAS, C. A. FYFE, S. RAMDAS, J. KLINOWSKI, AND G. C. GOBBI, *J. Phys. Chem.* **86** (1982), in press.
46. T. RAYMENT AND J. M. THOMAS, submitted.
47. G. R. MILLWARD AND J. M. THOMAS, submitted.
48. A. K. CHEETHAM, C. A. FYFE, J. V. SMITH, AND J. M. THOMAS, *J. Chem. Soc. Chem. Commun.* (1982), in press.
49. A. K. CHEETHAM, M. A. EDDY, J. M. THOMAS, AND D. A. JEFFERSON, *Nature (London)* (1982), in press.
50. A. K. CHEETHAM, J. M. THOMAS, M. A. EDDY, J. KLINOWSKI, AND M. W. ANDERSON, submitted.